

LDA Measurement in Roughness Sub-layer beneath Turbulent Boundary Layer

Developed over Two-dimensional Square Rough Surface

by

T. Kameda⁽¹⁾, S. Mochizuki⁽²⁾ and H. Osaka⁽³⁾

Yamaguchi University

Department of Mechanical Engineering

Tokiwadai 2-16-1, Ube 755-8611; Japan

⁽¹⁾E-Mail: kameda@yamaguchi-u.ac.jp

⁽²⁾E-Mail: shinsuke@yamaguchi-ac.jp

⁽³⁾E-Mail: ohsaka@yamaguchi-ac.jp

ABSTRACT

The roughness sublayer beneath the turbulent boundary layer that develops over three rough surfaces is investigated by laser Doppler anemometry (LDA). Three configurations of rough surfaces are examined, with square roughness elements arranged with roughness pitch ratio $P (= (b + w) / k)$, where b is groove width, w is roughness element width and k is roughness element height) of 3, 4 and 8 (see Fig. 1(a)), in order to investigate the transition from a d-type rough surface to k-type. The experiments are performed at Reynolds numbers, based on momentum thickness $R_\theta (= U_1 \theta / \nu)$ and roughness height $k^+ (= u_\tau k / \nu)$, exceeding 500 and 60 respectively. The representative scales of velocity and length for the separated free shear layer, defined based on the statistics of the inflectional mean velocity form in the roughness sublayer, are found to depend on the roughness pitch ratio. The curvature of the divided mean streamline and the development of a separated free shear layer result in momentum fluxes on the mean flow and turbulence at the $y_T = 0$ surface between the groove and the boundary layer. The pressure and friction drag coefficients ($\langle c_{DP} \rangle$ and $\langle c_{DV} \rangle$) per roughness pitch length are calculated by integrating the momentum equation, and the sum of these coefficients gives the average local skin friction coefficient $\langle c_f \rangle$. Pressure drag acting on a roughness element represents the dominant contribution to wall shear stress at roughness pitch ratios of greater than 4 (see Fig. 1(b)). Finally, it is shown that the pressure drag coefficient can be scaled based on the turbulent velocity and the length scale of the separated free shear layer.

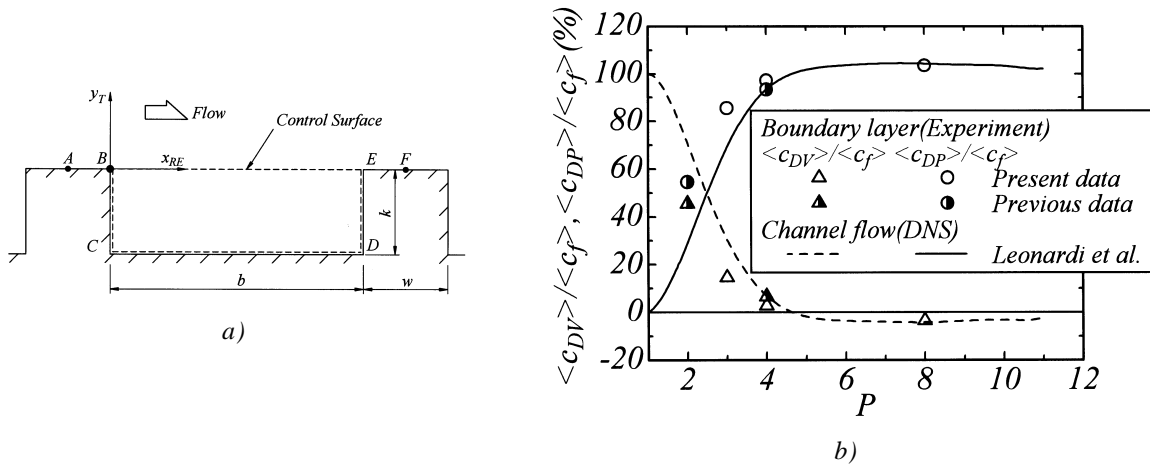


Fig. 1. Drag coefficient acting on a roughness pitch length.

(a) Control surface for calculation of momentum balance.

(b) Drag coefficient as a function of roughness pitch ratio.

1. INTRODUCTION

The turbulent boundary layer that develops over model rough surfaces has been investigated by many researchers in terms of the classification of rough surfaces (Perry et al., 1969) and the characteristics of streamwise mean velocity and turbulence of the various layers (see, e.g., Osaka et al., 1984; Tani, 1987; Wood and Antonia, 1975; Antonia and Luxton, 1971; Pineau et al., 1987; Kameda et al., 1998). Perry et al. (1969) classified rough surfaces constructed from a series of roughness elements of square cross-section as either d-type or k-type. The k-type surfaces are those on which the roughness elements are separated by a sufficient gap such that error in origin d_0 is related linearly to the roughness height. In contrast, the d-type surfaces have elements that are arranged so close that d_0 is proportional to the streamwise distance or the boundary layer thickness. These features might be related to the flow characteristics in the roughness sublayer over the rough surface.

The flow patterns in the roughness sublayer have been observed by Liu et al. (1966) and Morris (1959). In the case of small roughness pitch ratios, the flow separated by upstream roughness elements reattaches to the front wall of the downstream roughness element, whereas at large roughness pitch ratios, the flow reattaches to the surface between the roughness elements. Morris (1959) classified the flow over rough surfaces into quasi-smooth turbulent flow, hyper-turbulent flow and semi-smooth turbulent flow based on the behavior of the separated free shear layer formed behind the roughness element in the sublayer. The development of the separated free shear layer depending on the roughness pitch ratio may be one of the main factors responsible for drag acting on the roughness element.

Only a few quantitative studies of the roughness sublayer have been performed for a series of square roughness elements (Djenidi et al., 1999; Leonardi et al., 2003). The lack of investigative study on the roughness sublayer can be primarily attributed to the difficulty of measurement, which is complicated by reverse flow and intense turbulence. However, recent advancements in laser techniques have made it possible to measure the velocity field in the roughness sublayer. In the present study, the velocity components in the roughness sublayer beneath the turbulent boundary layer that develops over three rough surfaces are measured using a laser Doppler anemometry (LDA) system. The flow patterns and behavior of the separated free shear layer are investigated for three roughness pitch ratios and related to the magnitude of the wall shear stress.

2. EXPERIMENTAL SET UP AND CONDITONS

2.1 Experimental Set Up

Experiments were conducted in a closed-circuit open channel with test section of $400 \times 400 \text{ mm}^2$ and length of 1860 mm. An array of square bars with $10 \times 10 \text{ mm}^2$ cross-section (see Fig. 2) were placed as square roughness elements with a leading flat surface of 150 mm in length to allow the development of a smooth boundary layer. Different geometries of rough surface were chosen in terms of the roughness pitch ratio $P = (b + w) / k$, where b is the groove width, w is the element width, and k is the element (roughness) height. P of 3, 4 and 8 were examined. In order to obtain a smooth transition to the turbulent boundary layer, a tripping device constructed of 5 mm tripping wire and #5 mesh were placed over the leading surface for the smallest roughness pitch ratio of $P = 3$. The configuration with $P = 3$ was expected to exhibit transient properties from d-type to k-type roughness, whereas the higher ratios would be characteristic of k-type roughness based on previous research (see, e.g., Antonia and Luxton, 1971; Pineau et al., 1987; Kameda et al., 1998). The local skin friction coefficient will be highest at $P = 8$. The geometries of the rough surfaces are listed in Table 1. As shown in Figure 2, the surface between two of the roughness elements was replaced with a 0.14 mm-thick glass plate in order to measure the velocity components in this region in detail.

Instantaneous velocity measurements were made using a two-component LDA system (IFA-750, TSI). With the beam configuration used in the experiments, the volume of the crossing ellipsoid was $0.09 \times 0.13 \times 0.13 \text{ mm}^3$. High- and low-pass filters were set at 10 and 100 kHz. The detectable range of velocity measurement in this configuration was -14 to $+18 \text{ cm/s}$. The coincidence window width was determined to be 10 ms in a preliminary experiment. Nylon particles of $4 \text{ }\mu\text{m}$ diameter and specific gravity of 1.02 g/cm^3 were used as seeding particles. The sampling rate was 100–250 Hz, and a total of 100000 samples were taken.

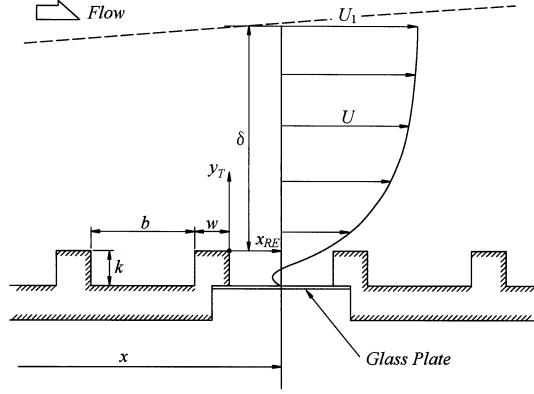


Fig. 2. Schematic showing flow field, coordinate system and nomenclature

Table 1. Geometries of the three rough surfaces

Roughness pitch ratio P	Element height k (mm)	Element width w (mm)	Groove width b (mm)
3	10	10	20
4	10	10	30
8	10	10	70

2.2 Experimental Conditions

The experimental conditions are listed in Table 2. The Reynolds number with respect of momentum thickness θ is given by $R_\theta = U_1 \theta / \nu$, where ν is the kinetic viscosity and U_1 is the free stream velocity, and satisfies a turbulent boundary layer over a smooth surface in the lowest limit (Purtell et al., 1981). The roughness Reynolds number is given by $k^+ = k u_\tau / \nu$, where u_τ is the friction velocity, and in the present case almost reaches the fully rough regime. In the open channel, the boundary layer is exposed to a favorable pressure gradient. The non-dimensional pressure gradient parameter is given by $K = (\nu / U_1^2) dU_1 / dx$, where x is the streamwise distance from the upstream roughness element of rough surface, and under these conditions represents a weak pressure gradient based on the empirical suggestion by Kline (1967). In the table, δ is the boundary layer thickness. The local skin friction coefficient is calculated from the momentum balance as follows.

$$c_f = 2 \frac{d\theta}{dx} + \frac{2\theta}{U_1} \frac{dU_1}{dx} \quad \text{----- (1)}$$

Table 2. Experimental conditions

P	x (mm)	U_1 (m / s)	R_θ	k^+	k / δ	K	c_f
3	915	9.71	630	63	0.19	2.49×10^{-11}	0.0083
4	805	9.50	700	85	0.20	6.58×10^{-11}	0.0160
8	765	9.64	890	112	0.15	6.65×10^{-11}	0.0272

3. RESULTS AND DISCUSSION

3.1 The mean flow characters throughout layers over three rough surfaces

Figures 3(a) and (b) show the profiles of streamwise mean velocity U and Reynolds shear stress $-\overline{uv}$ against vertical height y ($= y_T + d_0$) normalized by U_1 and δ . The measurements were made at the mid point ($x_{RE} / b = 0.5$) between the roughness elements. These figures include the data for a roughness pitch ratio of 2 ($R_\theta \cong 800$ and $k^+ \cong 60$) presented

by Liu et al. (1966). For the normalized streamwise mean velocity in Figure 3(a), the momentum deficit in the layer increases with increasing roughness pitch ratio. This tendency for the momentum deficit corresponds to an increase in the local skin friction with increasing roughness pitch ratio. The normalized Reynolds shear stress profiles peak in the vicinity of the rough surface, and the peak value increases with the roughness pitch ratio.

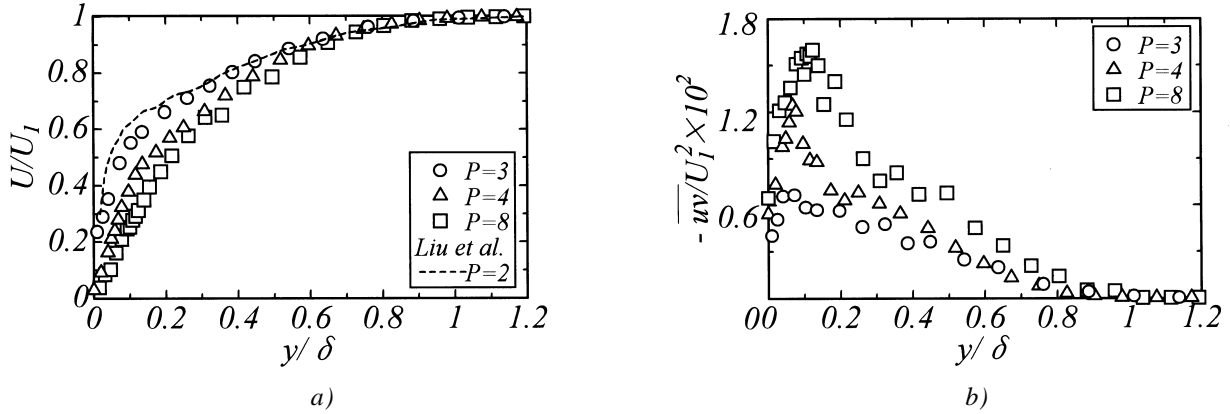


Fig. 3. Mean flow characteristics over the rough surfaces.

- (a) Streamwise mean velocity profiles.
- (b) Reynolds shear stress profiles.

3.2 Mean flow characteristics over one pitch length

Figures 4 and 5 show the profiles of streamwise mean velocity and Reynolds shear stress at several non-dimensional streamwise distances x_{RE}/b , normalized by u_τ and k . In the groove, the normalized mean velocity profiles take an inflectional form near a level equal to the top of the roughness elements ($y_T/k = 0$) with the formation of a separated shear layer. At the inflection point, the normalized velocity gradient $\partial(U/u_\tau)/\partial(y_T/k)$ decreases with increasing roughness pitch ratio. Negative streamwise mean velocity (i.e., reverse flow) can be recognized within the groove. As the roughness pitch ratio is increased, the development of the separated shear layer results in a smaller area and smaller magnitude of reverse flow in the groove. The Reynolds shear stress profile has a large peak near the inflection point in the mean velocity profile, obviously related to the development of the separated free shear layer through interaction between fluid inside the groove and boundary layer flow. Flow visualization by Djenidi et al. (1999), Townes and Sabersky (1966) and in a preliminary experiment of the present study confirmed the interaction that may produce the peaks in Reynolds shear stress over the groove.

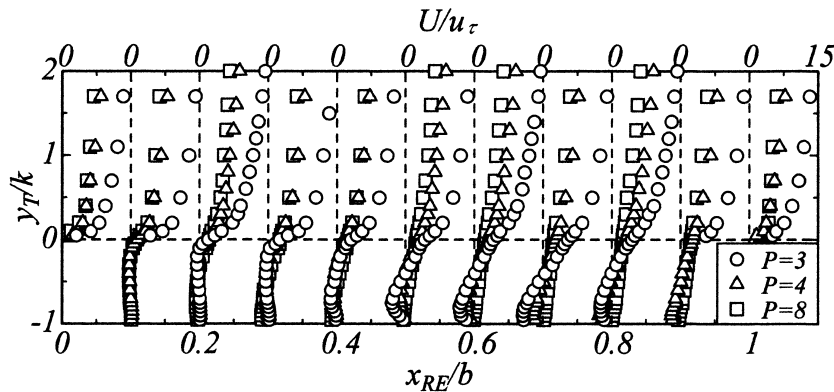


Fig. 4. Streamwise mean velocity profiles over roughness elements and in grooves at three different roughness pitch ratios

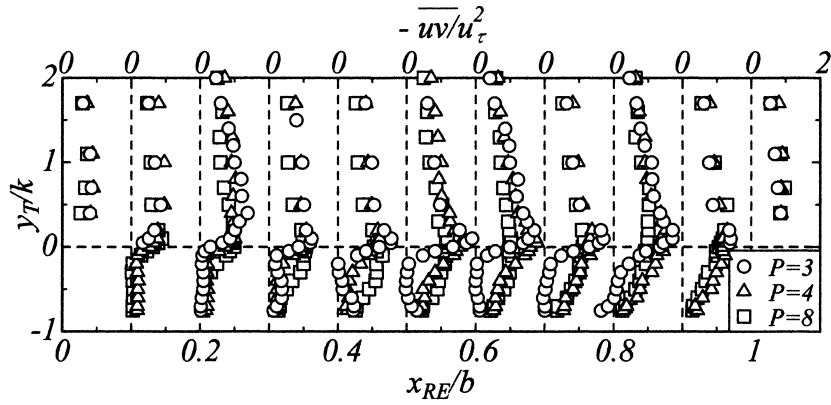


Fig. 5. Reynolds shear stress profiles over roughness elements and in grooves at three different roughness pitch ratios

3.3 Mean streamline inside groove

Mean streamlines were calculated from the measured streamwise and vertical mean velocities assuming a two-dimensional flow. The results are shown in Figures 6(a) to (c) for the stream function normalized by u_τ and k . At roughness pitch ratios of 3 and 4, the divided streamline that separated from the downstream edge of the upstream roughness element reattaches near the upstream edge of the downstream roughness element, and re-circulating flow exists near the upstream corner of the groove. At a roughness pitch ratio of 8, the divided mean streamline attaches at the bottom of the groove, and re-circulating flow occurs near both the upstream and downstream corners. Accordingly, the curvature of the mean streamline differs according to the roughness pitch ratio.

The centrifugal force U_t^2 / r per unit mass acting on the curvature of the mean streamline was calculated for the divided mean streamline. U_t is tangential velocity and r is radius of curvature. The results are shown in Figure 7 normalized by u_τ and k . The normalized centrifugal force decreases with increasing roughness pitch ratio, reaching almost zero at $P = 8$, indicating that the curvature of the mean streamline has less effect compared to the local skin friction coefficient.

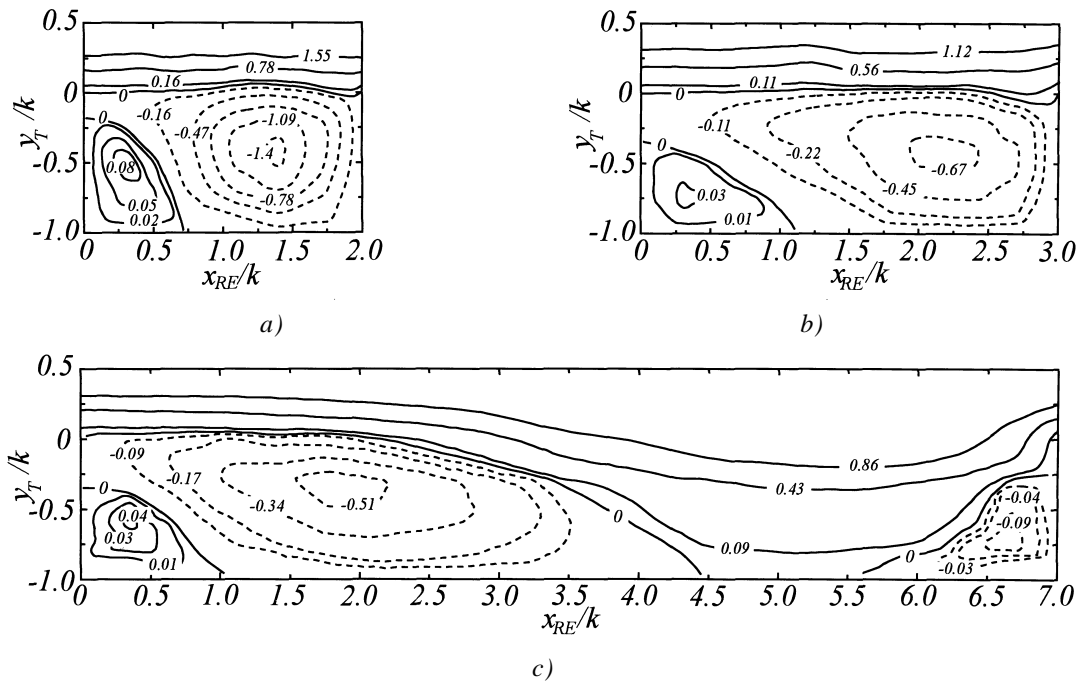


Fig. 6. Mean streamline in a groove at roughness pitch ratios of (a) 3, (b) 4 and (c) 8.

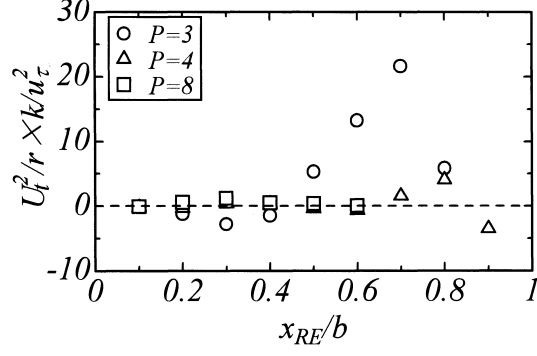


Fig. 7. Centrifugal force due to curvature of mean streamline.

3.4 Behavior of a separated free shear layer

Figures 8(a) to (d) show the representative scales based on the inflectional velocity form of the separated free shear layer. The central position $y_T|_{\max}$ of the separated free shear layer normalized by k (Fig. 8(a)) is defined as the height of the inflection point in the streamwise mean velocity profile. The central position is positive in the upstream region and negative in the downstream region. At a roughness pitch ratio of 8, the central position tends to shift downward due to reattachment of the divided mean streamline to the bottom of the groove. In Figure 8(b), the streamwise mean velocity at $y_T|_{\max}$, U_S , remains almost constant, except for regions near the upstream and downstream roughness elements over the groove, and takes smaller values with increasing roughness pitch ratio. In contrast to the streamwise mean velocity, the Reynolds shear stress at $y_T|_{\max}$ in Figure 8(c) does not exhibit a systematic variation with respect to the roughness pitch ratio. In Figure 8(d), the width b_S of the separated free shear layer normalized by k , defined as the distance between the heights of 0.5 and 1.5 times U_S , grows linearly with non-dimensional streamwise distance x_{RE}/b , except immediately adjacent to the downstream roughness element. A maximum value of $x_{RE}/b \approx 0.7$ is reached with increasing roughness pitch ratio.

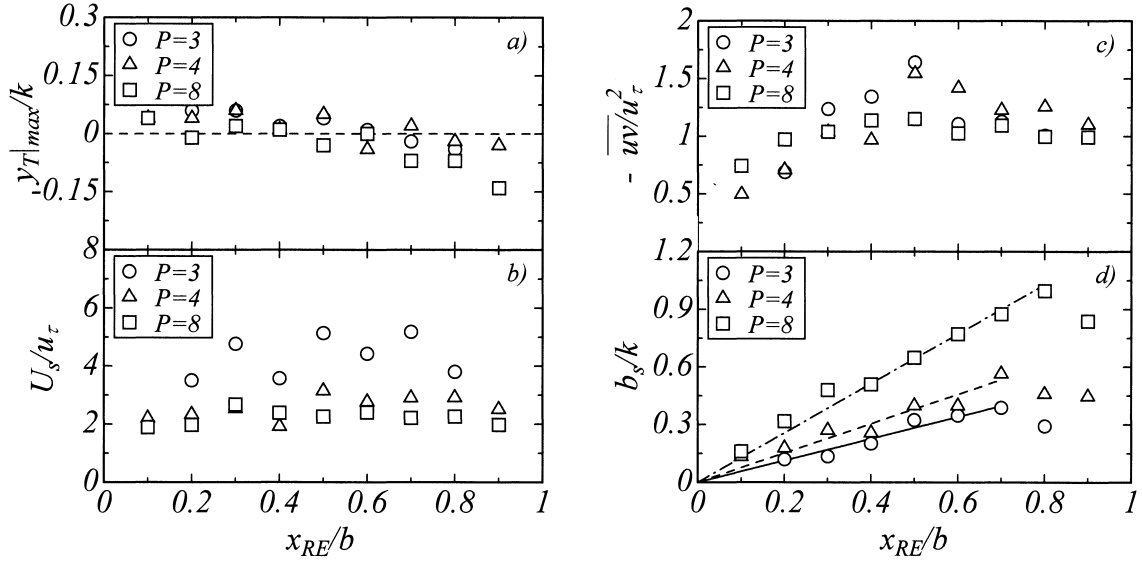


Fig. 8. Representative scales of separated free shear layer.

- (a) Central position of the separated free shear layer.
- (b) Streamwise mean velocity at the central position.
- (c) Reynolds shear stress at the central position.
- (d) Width of the separated free shear layer.

3.5 Momentum transport at the surface dividing boundary layer and groove

Figures 9(a) to (c) show the streamwise and vertical mean velocities and momentum flux normalized by u_τ at the $y_T = 0$ surface over the groove. The streamwise mean velocity profile reveals acceleration and deceleration in the region adjacent to the upstream and downstream roughness elements, respectively, representing the effects of wall restraint by the roughness elements. The maximum value at the $y_T = 0$ surface decreases with increasing roughness pitch ratio. The vertical mean velocity profile is closely related to the roughness pitch ratio as a response to the curvature of the mean streamline (see Fig. 6). With increasing the roughness pitch ratio, the vertical mean velocity changes from positive to negative in the central region at the $y_T = 0$ surface, and from negative to positive in the downstream region. The momentum flux of the mean flow, given by the product of the streamwise and vertical mean velocities, is produced by the curvature of the mean streamline. This result shows that the curvature contributes to momentum transport between the boundary layer and the groove.

Figures 9(d) to (f) show the streamwise and vertical turbulent intensities and Reynolds shear stress normalized by u_τ at the $y_T = 0$ surface over the groove. The magnitude of all components increases along development of the separated free shear layer. The existence of Reynolds shear stress (see Fig. 9(f)) contributes to the momentum transport at the $y_T = 0$ surface.

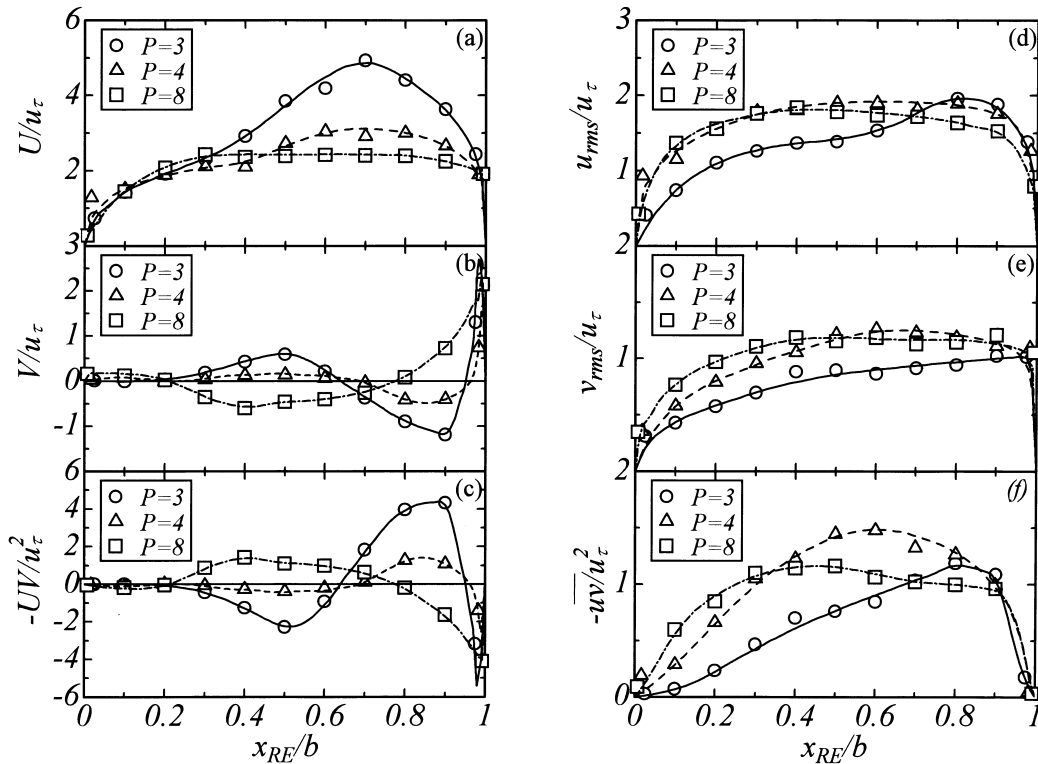


Fig. 9. Mean velocities and turbulence at the surface between the boundary layer and the groove.

- (a) Streamwise mean velocity.
- (b) Vertical mean velocity.
- (c) Momentum flux on mean flow due to curvature of the mean streamline.
- (d) Streamwise turbulent intensity.
- (e) Vertical turbulent intensity.
- (f) Reynolds shear stress.

3.6 Drag coefficients acting on a roughness element

For the control volume given in Figure 10, the pressure drag coefficient $\langle c_{DP} \rangle$ and the friction drag coefficient $\langle c_{DV} \rangle$ acting on a roughness pitch length $\lambda (=b+w)$ can be calculated by integration of momentum in the x direction, as follows.

$$\langle c_{DP} \rangle = \frac{2}{U_1^2 \lambda_B} \int_A^E [-UV] dx_{RE} + \frac{2}{U_1^2 \lambda_B} \int_B^E [-uv] dx_{RE} + \frac{2}{U_1^2 \lambda_B} \int_B^E \left[v \frac{\partial U}{\partial y_T} \right] dx_{RE} - \frac{2}{U_1^2 \lambda_C} \int_C^D \left[v \frac{\partial U}{\partial y_T} \right] dx_{RE}, \text{-----(2)}$$

and

$$\langle c_{DV} \rangle = \frac{2}{U_1^2 \lambda_A} \int_A^B \left[v \frac{\partial U}{\partial y_T} \right] dx_{RE} + \frac{2}{U_1^2 \lambda_C} \int_C^D \left[v \frac{\partial U}{\partial y_T} \right] dx_{RE} + \frac{2}{U_1^2 \lambda_E} \int_E^F \left[v \frac{\partial U}{\partial y_T} \right] dx_{RE}. \text{-----(3)}$$

The local skin friction coefficient $\langle c_f \rangle$ averaged per roughness pitch length λ is the sum of the two coefficients. Table 3 shows the results for each term of equations (2) and (3) calculated from experimental data. The maximum imbalance between $\langle c_f \rangle$ and c_f shown in table 2 is 14%, occurring at a roughness pitch ratio of 3. Using the data in the Table 3, Figure 11 compares direct numerical simulation (DNS) data for a two-dimensional channel by Leonardi et al. (2003) with the results of the present experiments and previous wind tunnel experiments ($P = 2$ and 4) involving direct measurement of the wall shear stress (Kameda et al., 2000). The experimental data is in qualitative agreement with the DNS results. As the roughness pitch ratio increases, the pressure drag contribution to the wall shear stress increases, reaching almost 100% of the wall shear stress of the rough surface at a roughness pitch ratio of more than 4. Below this value, the viscous stress contribution decreases and vanishes. Over square roughness elements, the pressure drag on the roughness element is the dominant contributor to the wall shear stress.

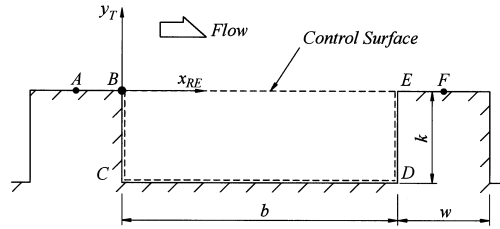


Fig. 10. Control surface for calculation of momentum balance using equations (2) and (3)

Table 3. Contributions to the local friction coefficient

P	$\langle c_{DP} \rangle \times 1000$				$\langle c_{DV} \rangle \times 1000$			$\langle c_f \rangle \times 1000$
	1 st term	2 nd term	3 rd term	4 th term	1 st term	2 nd term	3 rd term	
3	1.395	3.340	1.902	1.473	0.984	-1.473	1.855	9.48
4	0.801	11.904	1.611	1.843	0.939	-1.843	1.360	16.62
8	1.929	12.731	1.055	1.578	0.356	-1.578	0.329	25.40

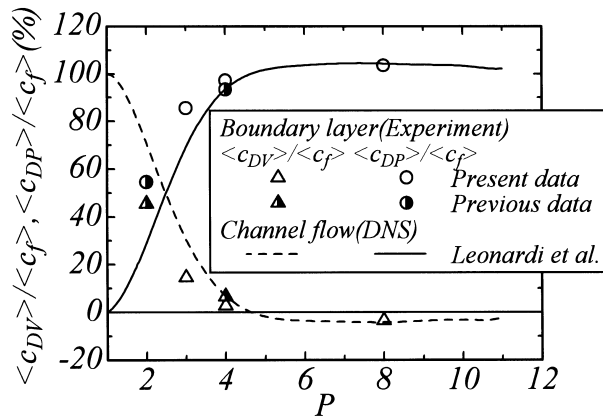


Fig. 11. Drag coefficients as a function of roughness pitch ratio.

3.7 The scaling of pressure drag coefficient

The pressure drag D_p per unit spanwise length can be approximated as the normal force acting on the sidewall of a roughness element, which in turn is defined in terms of the product of pressure and area per unit spanwise length on which the pressure acts. The order of magnitude of the pressure and area can be estimated from the velocity u and length scale ℓ of the separated free shear layer. D_p is then given as follows.

$$D_p = O \cdot \rho u^2 \ell, \quad \text{----- (4)}$$

where O means the order of magnitude and ρ is the density of fluid. The pressure drag coefficient $\langle c_{DP} \rangle$ per roughness pitch length λ can be estimated by

$$\langle c_{DP} \rangle = \frac{D_p}{1/2 \cdot \rho U_1^2 \lambda} \sim \frac{\rho u^2 \ell}{1/2 \cdot \rho U_1^2 \lambda} = 2 \frac{u^2}{U_1^2} \frac{\ell}{\lambda} \frac{k}{w+b} = 2 \frac{u^2}{U_1^2} \frac{\ell}{k} \frac{1}{P} \quad \text{----- (5)}$$

The length scale ℓ can be scaled with the width b_s of the separated free shear layer. However, for the mean velocity and turbulence fields of the separated free shear layer, there are two velocity scales; the mean velocity U_s of the separated free shear layer given the scale of dynamic pressure, and the turbulent intensity $(u_{rms})_s$ at $y_T|_{\max}$ interpreted as the scale of fluctuation pressure. In order to determine the most appropriate velocity scale for the pressure drag coefficient, the magnitude of the pressure drag coefficient was calculated using equation (5) at the scale of $x_{RE}/b = 0.7$, at which b_s is near its maximum Table 4 shows the relative values of the pressure drag coefficient for each roughness pitch ratio compared to $P = 3$. These results indicate that the velocity scale of turbulence field is suitable for scaling the pressure drag coefficient.

Table 4. Relative pressure drag coefficient

$\langle c_{DP} \rangle$	$\langle c_{DP} \rangle _{P=3} : \langle c_{DP} \rangle _{P=4} : \langle c_{DP} \rangle _{P=8}$
Experimental results in the table 3	1 : 2 : 3.2
Mean flow field	
$2 \frac{U_s^2}{U_1^2} \frac{b_s}{k} \frac{1}{P}$	1 : 0.68 : 0.54
Turbulence field	
$2 \frac{(u_{rms})_s^2}{U_1^2} \frac{b_s}{k} \frac{1}{P}$	1 : 2.1 : 2.8

4. SUMMARY

The roughness sublayer beneath the turbulent boundary layer over three rough surfaces formed by square roughness elements was investigated by laser Doppler anemometry. The flow patterns over three roughness pitch ratios were quantitatively described in mean streamlines calculated using the mean velocity components. At roughness pitch ratios of 3 and 4, the divided mean streamline that separated from the downstream edge of the upstream roughness element was found to reattach at the upstream edge of the downstream roughness element. However, at a roughness pitch ratio of 8, the divided streamline attaches to the bottom of the groove in front of the downstream roughness element. Re-circulating flows form around both the upstream and downstream corners of the groove. The pressure drag coefficient acting on the rough surface was estimated considering the control surface in the roughness sublayer, and it was found that the pressure drag contribution to the wall shear stress increases with the roughness pitch ratio to reach almost 100% at roughness pitch ratios of 4 or greater. From the velocity and length scales defined in the separated free shear layer, it was confirmed that the velocity scale of turbulence field is suitable for scaling the pressure drag coefficient.

ACKNOWLEDGMENT

The authors gratefully acknowledge to ‘‘The Mazda Foundation’’ for the support of research grant.

REFERENCES

- Antonia R.A. and Luxton R.E. (1971), "The Response of a Turbulent Boundary layer to a Step Change in surface Roughness: Part 1. Smooth to Rough", *J. Fluid Mech.*, 48-4, pp. 721-761.
- Djenidi L., Elaverasan R. and Antonia R.A. (1999)," The Turbulent Boundary Layer over Transverse Square Cavities", *J. Fluid Mech.*, 395, pp.271-294.
- Kameda T., Osaka H. and Mochizuki S. (1998), " Mean Flow Quantities for the Turbulent Boundary Layer over a k-type Rough Wall", 13TH Australasian Fluid Mechanics Conference, Monash Uni., Melbourne, Australia, pp.357-360.
- Kameda T., Osaka H. and Mochizuki S. (2000), "Turbulent Structure in the Vicinity of a Roughness Element for Boundary Layer over a k-Type Rough Wall", *Transaction of JSME, Series B*, 66-646, pp.1347-1355.
- Leonardi S., Orlandi P., Smalley R.J., Djenidi L. and Antonia R.A. (2003), "Direct Numerical Simulations of Turbulent Channel Flow with Transverse Square Bars on One Wall", *J. Fluid Mech.*, 491, pp.229-238.
- Liu C.K., Kline S.J. and Johnston J.P. (1966), "An Experimental Study of Turbulent Boundary Layer on Rough Walls", *Stanford Univ. Mech. Eng., Rep.MD-15*.
- Morris H.H. (1959), " Design Methods for Flow in Rough Conditions", *Proc. ASCE, J. Hyd. Div.*, 85-HY7, pp.43-62.
- Osaka H., Nakamura I. and Kageyama Y. (1984), Mean Flow Quantities for the Turbulent Boundary Layer over a d-Type Rough wall, *Transaction of JSME, Series B*, 50-458, pp.2299-2306.
- Perry A.E., Schofield W.H. and Joubert P.N. (1969), "Rough Wall Turbulent Boundary Layer", *J. Fluid Mech.*, 37-2, pp.383-413.
- Pineau F., Nguyen V.D., Dickinson J. and Belanger I (1987), " Study of Flow over a Rough Surface with Passive Boundary layer Manipulators and Direct Wall Drag Measurements", *AIAA Paper, No.87-0357*.
- Purtell L.P., Klebano P.S. and Buckley F.T.(1981), "Turbulent Boundary Layer at Low Reynolds Number", *Phys. Fluids*, 24-5, pp.802-811.
- Tani I.(1987), "Turbulent Boundary Layer Development over Rough Surface", *Perspective in Turbulence Studies*, Editor; Meier H.U. and Bradshaw P., Springer-Verlag, pp.223-249.
- Townes H.W. and Sabersky R.H. (1966), "Experiments on the Flow over a Rough Surface", *J. Heat Mass Transfer*, 9, pp.729-738.
- Wood D.H.and Antonia R.A. (1975), "Measurements in a Turbulent Boundary Layer over a d-Type Surface Roughness", *Trance. ASME, Series E, J. App. Mech.*, 42-3, pp.591-597.